Aberystwyth University

Expression of FlHMA3, a vacuolar P1B2-ATPase from Festulolium loliaceum, correlates with response to cadmium stress

Guo, Qiang; Meng, Lin; Humphreys, Mike W.; Scullion, John; Mur, Luis A.J.

Accepted Manuscript

Expression of *FlHMA3*, a vacuolar P_{1B2}-ATPase from *Festulolium loliaceum*, correlates with response to cadmium stress

Qiang Guo, Lin Meng, Mike W. Humphreys, John Scullion, Luis A.J. Mur

Please cite this article as: Q. Guo, L. Meng, M.W. Humphreys, J. Scullion, L.A.J. Mur, Expression of *FlHMA3*, a vacuolar P_{1B2}-ATPase from *Festulolium loliaceum*, correlates with response to cadmium stress, *Plant Physiology et Biochemistry* (2017), doi: 10.1016/j.plaphy.2017.01.013.

1 **Title:** Expression of *FlHMA3*, a vacuolar P_{1B2}-ATPase from *Festulolium loliaceum*,

2 correlates with response to cadmium stress

3 **Authors:** Qiang Guo[a], Lin Meng[a]*, Mike W. Humphreys[b], John Scullion[b], Luis A. J.

4 Mur[b]

5 **Institutional addresses:** [a] Beijing Research and Development Center for Grass and

6 Environment, Beijing Academy of Agriculture and Forestry Science, Beijing 100097, P.

7 R. China; [b] Institute of Biological, Environmental and Rural Sciences, Aberystwyth

8 University, Aberystwyth SY23 3DA, UK

9 [*]**Corresponding author:** Lin Meng; E-mail: menglin9599@sina.com

10 **Tel:** +86-10-51503345

11 **Fax:** +86-10-51503297

12

13

14

15

16

17

18

19

20

21

22

1 **Abstract**

2   Heavy metal ATPase 3 (HMA3), a P_{1B2}-ATPase, is a key tonoplast transporter

3 involved in mediating the vacuolar sequestration of cadmium (Cd) to detoxify the

4 intake of this element by plants. HMA3 expression in response to Cd stress has not

5 been previously examined in the grass hybrid species *Festulolium loliaceum* (Huds.) P.

6 Fourn. In this study, *FlHMA3* isolated from *F. loliaceum* was found to comprise 833

7 amino acid residues with 77% homology to the rice *OsHMA3*. Transient expression of

8 *FlHMA3* fused to enhanced green fluorescent protein in Arabidopsis protoplasts

9 suggested its localization to vacuolar membranes. Quantitative real-time RT-PCR

10 analysis of *F. loliaceum* revealed that *FlHMA3* is expressed predominantly within

11 roots and up-regulated by excess Cd. Over the 168 h treatment, Cd content of *F.*

12 *loliaceum* roots was significantly higher than that of shoots, regardless of external

13 $CdCl_2$ concentrations. A significant positive correlation was found between *FlHMA3*

14 expression and Cd accumulation in roots of *F. loliaceum* seedlings subjected to

15 10–100 mg L^{-1} $CdCl_2$ for 168 h or, in a separate experiment, to 25 or 100 mg L^{-1}

16 $CdCl_2$ for the same duration. These findings provide evidence that *FlHMA3* encodes a

17 vacuolar P_{1B2}-ATPase that may play an important role in Cd^{2+} sequestration into root

18 cell vacuoles, thereby limiting the entry of Cd^{2+} into the cytoplasm and reducing Cd^{2+}

19 toxicity.

20 **Keywords:** cadmium, *Festulolium loliaceum*, *FlHMA3*, phytomediation, vacuole

21 sequestration

22

1. Introduction

An expanding global population and the limited availability of agriculturally suitable land have stimulated interest in the agricultural potential of more marginal areas and contaminated "brown-field" locations on former industrial sites. Of the estimated 30,000 t of Cd released annually into the environment, 13,000 t are due to human activity (Gallego et al., 2012). A non-essential heavy metal with high toxicity to plants, Cd interferes with the homeostasis of essential elements such as zinc, calcium, and iron and initiates their displacement from proteins (Verbruggen et al., 2009; Guo et al., 2014). Cd contamination of soil has become a serious environmental concern and also threatens human health via its accumulation in the food chain (Satoh-Nagasawa et al., 2012). Crops and products derived from livestock raised on plant-based diets are important sources of heavy metals absorbed by humans (Peralta-Videa et al., 2009). Understanding the mechanism of Cd accumulation in plants and the factors affecting its deposition are crucial to reduce entry of Cd into the human food chain.

Plants have evolved alternative adaptation strategies to cope with Cd stress. One such mechanism involves production of phytochelatins (PCs), which are glutathione-derived peptides. PCs are synthesized in the cytosol, where they form PC-Cd complexes that are subsequently sequestered into vacuoles to reduce the deleterious effects of Cd accumulation in the cytosol (Mendoza-Cózatl et al., 2005; Clemens, 2006). This process plays an important role in heavy metal homeostasis and detoxification (Colangelo and Guerinot, 2006; Hanikenne and Nouet, 2011). Generally, vacuolar sequestration of Cd^{2+} can be mediated by heavy metal

3

1   transporters in plants (Hirschi et al., 2000; Song et al., 2003; Korenkov et al., 2007;

2   Wojas et al., 2009). Among these transporters are P_{1B}-ATPases (heavy metal

3   P_{1B}-ATPases, HMAs), a large group of ATP-driven pumps implicated in the transport

4   of monovalent Cu^+/Ag^+ (P_{1B1}-ATPases) and divalent $Zn^{2+}/Cd^{2+}/Co^{2+}/Pb^{2+}$

5   (P_{1B2}-ATPases) heavy metal cations across plant membranes (Williams and Mills,

6   2005). As is well known, HMAs are involved in removal of heavy metal ions from the

7   cytosol into either the apoplast, the vacuole, or into other organelles (Hussain et al.,

8   2004; Andrés-Colás et al., 2006; Kim et al., 2009). In *Arabidopsis thaliana*,

9   *AtHMA1-AtHMA4* and *AtHMA5-AtHMA8* transport divalent and monovalent cations,

10   respectively (Cobbett et al., 2003; Williams and Mills, 2005). *AtHMA3* belongs to the

11    $Zn^{2+}/Cd^{2+}/Co^{2+}/Pb^{2+}$ subgroup; localized in the tonoplast, it helps detoxify essential

12   biological (Zn^{2+}) and non-essential (Cd^{2+}, Co^{2+}, and Pb^{2+}) heavy metals by

13   participating in their vacuolar sequestration (Morel et al., 2009). *AtHMA3* is a major

14   locus in *A. thaliana* responsible for the regulation of Cd accumulation (Chao et al.,

15   2012). *AhHMA3* has high-level constitutive expression in *A. halleri*, a Zn

16   hyperaccumulator and relative of *A. thaliana*, which suggests that this gene is

17   involved in high Zn accumulation (Becher et al., 2004). Similarly, *TcHMA3* from

18   *Thlaspi caerulescens*, a Cd hyperaccumulator, is highly expressed in leaves; it plays

19   an important role in the detoxification of Cd by sequestering Cd into leaf vacuoles,

20   thereby contributing to Cd hyperaccumulation and hypertolerance (Ueno et al., 2011).

21   Among the nine *HMA* genes identified in rice is *OsHMA3*, a member of the

22    $Zn^{2+}/Cd^{2+}/Co^{2+}/Pb^{2+}$ subgroup (Miyadate et al., 2011; Takahashi et al., 2012).

4

1   *OsHMA3*, a tonoplast-localized transporter of Cd within root cells, plays a role in the

2   sequestration of Cd^{2+} into root cell vacuoles (Ueno et al., 2010). *OsHMA3* has been

3   identified as the locus responsible for regulation of Cd accumulation in shoots of rice

4   cultivars Anjana Dhan and Cho-Ko-Koku. When the function of this protein is lost,

5   Cd^{2+} passage through the xylem is increased, thereby leading to Cd^{2+} accumulation in

6   the shoots (Ueno et al., 2010; Miyadate et al., 2011). Sasaki et al. (2014) recently

7   found that overexpression of *OsHMA3* contributed to reduced Cd^{2+} accumulation in

8   the grain and to enhanced Cd tolerance in rice. Taken together, the available evidence

9   implies that *HMA3*-mediated vacuolar sequestration of heavy metals plays an

10 important role in metal detoxification.

11 *Festulolium* grass hybrids combine many of the attributes of *Lolium* species

12 (ryegrasses), such as high growth rates that provides high yields of nutritious,

13 palatable fodder for livestock, and those of *Festuca* species (fescues) which provide

14 resilience against different climatic and edaphic stresses (Humphreys et al., 2014).

15 Natural *Festulolium* species hybrids exist, especially in undisturbed marginal

16 grassland locations frequently exposed to stress conditions where productive *Lolium*

17 species would be more disadvantageous (Humphreys et al., 1995). A range of

18 synthetic *Festulolium* species hybrids are also being generated by grass breeders to

19 achieve productive, stress-adapted varieties suitable for agriculture, with safeguards to

20 assist withstanding various climatic conditions. The natural grass species hybrid

21 *Festulolium loliaceum* survives in waterlogged soils prone to flooding and its

22 synthetic varieties developed combat freezing temperatures or to mitigate incidents of

1   flooding (Macleod et al., 2013). *Festulolium loliaceum* was developed following the

2   hybridisation of *Lolium perenne* (perennial ryegrass) with *Festuca pratensis* (meadow

3   fescue). Eventhough *F. loliaceum* has been broadly recognized for its resilience to

4   stress conditions, studies in this regard have been primarily confined to climatic rather

5   than edaphic stresses; consequently, the potential use of this species for

6   bioremediation and its tolerance to Cd-contaminated soils have not been previously

7   explored. In this context, we isolated and characterized *FlHMA3* from *F. loliaceum*

8   and verified its subcellular localization. We also analyzed *FlHMA3* expression in

9   plants exposed to high Cd concentrations, which revealed patterns consistent with a

10   role in the conferral of heavy metal tolerance. Our findings provide useful initial

11   information on the potential future agricultural application of this grass hybrid on

12   Cd-contaminated soils.

13

1 **2. Materials and Methods**

2 *2.1 Plant growth conditions and treatments*

3   Seeds of *Festulolium loliaceum* variety Prior ($2n = 4x = 28$) were provided by the

4 Institute of Biological, Environmental, and Rural Sciences (IBERS), Aberystwyth

5 University. Seeds were sterilized with 5% sodium hypochlorite solution for 5 min,

6 rinsed thoroughly with distilled water, and then germinated on moistened filter paper

7 for 168 h at 25°C in dark. After emergence of plumules, uniform seedlings were

8 selected and transferred into plastic containers filled with 0.6 L modified Hoagland's

9 solution containing 2 mM KNO_3, 1 mM $NH_4H_2PO_4$, 0.5 mM $Ca(NO_3)_2 \cdot 4H_2O$, 0.5

10 mM $MgSO_4 \cdot 7H_2O$, 60 µM Fe-citrate, 92 µM H_3BO_3, 18 µM $MnCl_2 \cdot 4H_2O$, 1.6 µM

11 $ZnSO_4 \cdot 7H_2O$, 0.6 µM $CuSO_4 \cdot 5H_2O$, and 0.7 µM $(NH_4)_6Mo_7O_{24} \cdot 4H_2O$ for 5 weeks.

12 The nutrient solution was renewed every 2 d. All seedlings were grown in a CE

13 growth chamber under a 16 h/8 h day/night cycle at 25°C/18°C, a relative humidity of

14 50% to 60%, and a light intensity of 200 µmol m^{-2} s^{-1}. Five-week-old plants were

15 used for all treatments, with each treatment replicated eight times and each replicate

16 comprising five individual plants. Containers for all treatments were arranged in a

17 completely randomized block design. Two treatment approaches were used: (i)

18 Hoagland's nutrient solution supplemented with 0, 10, 25, 50, and 100 mg L^{-1} $CdCl_2$

19 for 168 h; and (ii) Hoagland's nutrient solution containing 25 or 100 mg L^{-1} $CdCl_2$,

20 with plants removed following 0, 3, 6, 12, 24, 48, 72, 96, 120, 144, and 168 h

21 exposure. These exposure concentrations were not selected to simulate field

22 conditions. Rather they were determined to observe Cd uptake and stress of the plants

23 over a short period of exposure in order to better understand plant mitigation

1 responses.

2 *2.2. Calculation of relative growth rate*

3 The relative growth rate (RGR) of whole plants was calculated using the formula

4 RGR = (lnWj− lnWi)/Δt, where Wi and Wj are dry weights before and after 168 h

5 treatment, respectively, and Δt is elapsed time between the two measurements

6 (Martínez et al., 2005).

7 *2.3. Cloning of FlHMA3*

8 Total RNA was extracted according to Guo et al. (2012) from roots of *F.*

9 *loliaceum* seedlings exposed to 100 mg L^{-1} $CdCl_2$ for 24 h. First-strand cDNA was

10 synthesized from 2 µg total RNA using an oligo(dT) primer and PrimeScriptRTase

11 (Takara). The partial cDNA fragment of *FlHMA3* was amplified by PCR using

12 degenerate primers P1 and P2 (Table S1) designed based on the gene sequences of

13 *BdHMA3* (*Brachypodium distachyon*, XM_003561234), *HvHMA3* (*Hordeum vulgare*,

14 KU212808), *OsHMA3* (*Oryza sativa*, XM_015791882), *TaHMA3* (*Triticum aestivum*,

15 KF683298), and *ZmHMA3* (*Zea mays*, XM_008671782). PCR cycling conditions

16 were as follows: 94°C for 2 min, followed by 30 cycles of 94°C for 30 s, 55°C for 30

17 s, and 72°C for 40 s, with a final extension at 72°C for 10 min. The PCR product was

18 purified from agarose gels, ligated into a pMD-19T vector (Takara), and sequenced by

19 Sangon Biotech (China). The 5′- and 3′-ends of *FlHMA3* were obtained with 5′- and

20 3′- Rapid Amplification of cDNA Ends kits (SMARTer RACE, Clontech) according

21 to the manufacturer's instructions and specific primers P3 and P4, respectively (Table

22 S1). These fragments were assembled to obtain the full-sequence of *FlHMA3* cDNA.

1   *2.4. Sequence analysis*

2   A BLAST search was performed using the NCBI platform

3   (http://www.ncbi.nlm.nih.gov/BLAST). Sequence analysis of cDNA and multiple

4   alignments were performed with DNAMAN 8.0 software. Molecular mass and

5   isoelectric point of the deduced protein encoded by *FlHMA3* was predicted using the

6   ExPASy proteomics server (http://www.expasy.org). Hydrophobicity values were

7   calculated using the program TMPRED available at http://www.ch.embnet.org/.

8   Phylogenetic relationship of *FlHMA3* with other plant *HMAs* multiple sequence

9   alignment was analyzed by multiple alignments using Clustal X software (Thompson

10   et al., 1997). Then a phylogenetic tree was constructed by MEGA6.0 software using

11   the neighbor-joining method with 1,000 bootstrap replicates (Tamura et al., 2011).

12   *2.5. Subcellular localization of FlHMA3*

13   The open reading frame (ORF) of *FlHMA3* excluding the stop codon was

14   amplified using PrimeSTAR HS DNA polymerase with primers P5 (Table S1, EcoRI

15   restriction site underlined) and P6 (Table S1, KpnI restriction site underlined), cloned

16   into a pMD-19T vector, and sequenced by Sangon Biotech. The amplified fragment

17   was cut from the pMD-19T plasmid using EcoRI and KpnI restriction enzymes and

18   cloned into a pBSHES-NL vector to generate a fusion with enhanced green

19   fluorescent protein (EGFP) under the control of the CaMV35S promoter. The

20   *FlHMA3*-GFP fusion construct or a non-GFP-tagged vector construct was transiently

21   expressed in protoplasts isolated from *A. thaliana* Col-0 cell suspensions using the

22   polyethylene glycol-mediated method (Yoo et al., 2007). Protoplasts containing the

1   plasmids were incubated at 23°C for 2–3 d in darkness. For FM4-64 staining,

2   protoplasts were transferred into 50 µM FM4-64 in Murashige-Skoog medium

3   containing 0.4 M mannitol for 10 min at 4°C according to the method of Ueda et al.

4   (2001). Fluorescent signals from both GFP and FM4-64 in the protoplasts were then

5   observed using an inverted Carl Zeiss LSM 710 confocal laser scanning microscope.

6   GFP and FM4-64 were excited at 488 nm and 543 nm, respectively, with their

7   corresponding fluorescence emission signals detected between 498–539 nm and

8   580–650 nm, respectively.

9   *2.6. Expression analysis of FlHMA3*

10   Total RNA was extracted with Trizol kit (Takara) following the manufacturer's

11   instructions. First-strand cDNA was synthesized from 2 µg of total RNA using an

12   oligo(dT) primer and PrimeScriptRTase (Takara). Quantitative real-time RT-PCR

13   (qRT-PCR) was performed using SYBR Premix Ex *Taq* II (Perfect Real Time) (Takara)

14   on a StepOnePlus Real-Time PCR system (ABI) to monitor the amplification of each

15   cDNA fragment. qRT-PCR amplification of *FlHMA3* was carried out with the primer

16   pair P7 and P8 (Table S1), which yielded a 225 bp product. For use as a reference in

17   the qRT-PCR, a 130 bp region of the *actin* gene was amplified using primers A1 and

18   A2, which were designed according to the partial cDNA sequence of *actin* from *F.*

19   *loliaceum* (Table S1). Primer sequences were designed with Primer 5.0 software. The

20   amplification protocol consisted of an initial denaturation step of 95°C for 10 min,

21   followed by 40 cycles of 95°C for 30 s, 60°C for 30 s, and 72°C for 30 s. Gene

22   expression data were normalized and relative expression was calculated by the $2^{-\Delta\Delta Ct}$

1 method (Livak and Schmittgen, 2001). Each experiment included three biological

2 replicates.

3 *2.7. Determination of Cd content*

4 Harvested plants were thoroughly washed with deionized water, divided into

5 shoots and roots, and oven dried at 80°C to a constant weight. Dried shoots and roots

6 were ground and digested in a mixture of $HNO_3/HClO_4$ (5/1, v/v) for 24 h and then

7 heated at 150–200°C to near dryness. After cooling, the residue was dissolved in

8 distilled deionized water to a total volume of 20 mL. Cd content was determined

9 using an atomic absorption spectrophotometer (AA-6300C, Shimadza, Kyoto, Japan).

10 *2.8. Statistical analysis*

11 All data were calculated as means plus standard deviation (SD). Statistical

12 analyses, one-way analysis of variance, and Duncan's multiple range tests comparing

13 treatment means were performed using SPSSv13.0 statistical software (SPSS Inc.,

14 Chicago, IL, USA).

15

16

17

18

19

20

21

22

1   **3. Results**

2   *3.1. Characterization of FlHMA3*

3   The full-length cDNA of *FlHMA3* isolated from roots was obtained by RT-PCR

4   and rapid amplification of cDNA ends. The sequence, which comprised 2,957 bp,

5   contained a 2,502 bp ORF encoding 833 amino acid residues with an estimated

6   molecular mass of 87.58 kDa and a theoretical isoelectric point of 5.33. As shown in

7   Fig. 1, multiple sequence alignment revealed that *FlHMA3* shares high homology

8   with amino acid sequences of orthologs *TaHMA3* from wheat (83%) and *OsHMA3*

9   from rice (77%) and, to a lesser extent, *AtHMA3* from *A. thaliana* (54%). This

10 similarity indicates that *F1HMA3* is a P_{1B2}-ATPase. A previous study has shown that

11 *OsHMA3* encodes a divalent metal ion (Cd^{2+}) transporter P_{1B2}-ATPase involved in

12 mediating the sequestration of Cd into vacuoles (Miyadate et al., 2011). Our

13 phylogenetic analysis placed *FlHMA3* into a clade with other *HMA3* genes from

14 closely related monocotyledonous species such as wheat (*TaHMA3*) and rice

15 (*OsHMA3*) (Fig. S1). These results suggest that *FlHMA3* encodes a P_{IB2}-ATPase

16 transporter.

17 Hydrophobicity plot analysis of the deduced polypeptide showed that *FlHMA3*

18 has eight transmembrane domains (Fig. 1, TM1 to TM8). Like all P-type ATPases, it

19 contains the characteristic motifs for an ATP binding (GDGxNDx), a phosphorylation

20 (DKTGTLT), and an HP locus forming a large cytoplasmic loop. Moreover, *FlHMA3*

21 possesses a CPC ion transduction motif in TM5, and a heavy-metal-associated domain

22 containing the motif GxCCxxE was located at the N terminus of *FlHMA3*.

23 *3.2. Transient expression of FlHMA3 in mesophyll protoplasts of Arabidopsis*

1   To determine the subcellular localization of *FlHMA3*, a GFP reporter construct

2   was developed to express a fusion protein consisting of GFP fused to the C terminus

3   of *FlHMA3* (FlHMA3:GFP) under the control of the CaMV35S promoter. This

4   construct was then transfected into mesophyll cells of *A. thaliana* protoplasts using

5   the polyethylene glycol method. Expression of the control (35S:GFP) resulted in

6   distribution of GFP signals throughout the cytoplasm and the nucleus of mesophyll

7   protoplasts (Fig. 2A). When FlHMA3:GFP was transfected into the protoplasts of

8   mesophyll cells, however, the GFP signals were clearly separated, with FM 4-64

9   signals in the area of the plasma membrane and tonoplast (Fig. 2B). This observation

10   suggests that *FlHMA3*, in line with its presumed function, is localized specifically on

11   the vacuolar membrane.

12   *3.3. Expression patterns of FlHMA3 in F. loliaceum exposed to Cd*

13   To investigate the effect of Cd on transcription of *FlHMA3*, plants were treated

14   with different concentrations of $CdCl_2$ for 168 h. As shown in Fig. 3A, mRNA levels

15   of *FlHMA3* were 2.2–6.6 folds higher in roots than in shoots at external $CdCl_2$

16   concentrations of 10–100 mg L^{-1}. Compared with the control, exposure to 10–100 mg

17   L^{-1} $CdCl_2$ led to significantly increased *FlHMA3* transcription in roots, with the

18   highest transcription levels observed with the most concentrated solution (100 mg L^{-1}

19   $CdCl_2$). The expression of *FlHMA3* was significantly lower in shoots and did not

20   change in response to the increase in $CdCl_2$ concentration.

21   To further determine the kinetics for Cd^{2+} induced activation of *FlHMA3* in

22   tissues, *FlHMA3* transcript levels were examined in plants exposed to 25 and 100 mg

13

1   L^{-1} CdCl$_2$ over a 168 h period. When exposed to 25 mg L^{-1} CdCl$_2$, *FlHMA3* transcript

2   levels increased gradually in both roots and shoots from 3 to 168 h, but the magnitude

3   was higher in roots than in shoots (Fig. 3B). In the case of 100 mg L^{-1} CdCl$_2$

4   treatment, *FlHMA3* transcript levels increased rapidly in both shoots and roots from 3

5   to 72 h; after peaking at 96 h, levels declined and remained constant following

6   exposure for 120–168 h. Under this treatment, *FlHMA3* expression was always higher

7   in roots than in shoots (Fig. 3C). Taken together, these results provide strong evidence

8   to suggest that *FlHMA3* at least within the 168 h timeframe used in this study is

9   expressed primarily in roots, with the extent of its transcription determined by the

10   level of CdCl$_2$ exposure.

11   *3.4. Cd accumulation in tissues and its relationship with the expression levels of*

12   *FlHMA3*

13   As external CdCl$_2$ concentrations were increased, Cd contents of shoots and roots

14   increased progressively after 168 h of growth; however, Cd contents of roots were

15   significantly higher than those of shoots at concentrations of 10–100 mg L^{-1} CdCl$_2$

16   (Fig. 4A). Moreover, an increase in CdCl$_2$ concentration from 50 to 100 mg L^{-1} had

17   no impact on Cd contents of shoots (Fig. 4A). We further observed a significant

18   positive correlation between Cd content and *FlHMA3* expression level in roots of *F.*

19   *loliaceum* exposed to 25–100 mg L^{-1} CdCl$_2$ for 168 h (Fig. 4B). Despite the increased

20   *FlHMA3* expression, however, the increase in Cd had a negative impact on plant

21   growth rate even though roots did not appear to be necrotic or changed in overall

22   length or branching and were therefore considered to be functional. A 14%–38%

1   reduction in relative growth rate compared with the control was recorded between the

2   treatment extremes (10–100 mg L^{-1} $CdCl_2$) (Fig. S2). Despite this effect the *F.*

3   *loliaceum* plants survived following the treatments without further evidence of

4   toxicity symptoms such as chlorosis or necrosis, consistent with our presumption that

5   root functionality was maintained.

6   To monitor the differences in Cd accumulation in root and shoot tissue over time,

7   we recorded changes in plants exposed to 25 or 100 mg L^{-1} $CdCl_2$ over a 168 h period.

8   The addition of either 25 or 100 mg L^{-1} $CdCl_2$ significantly increased Cd content in

9   both shoots and roots, but the content was always higher in roots than in shoots (Fig.

10   5A). In plants undergone 100 mg L^{-1} $CdCl_2$ treatment, the concentration of Cd in both

11   shoots and roots was significantly greater than in tissues exposed to 25 mg L^{-1} $CdCl_2$

12   from 3 to 168 h (Fig. 6A). In addition, we observed no significant difference in Cd

13   accumulation by shoots in the presence of either 25 or 100 mg L^{-1} $CdCl_2$ between 48

14   and 168 h (Figs. 5A–6A). A significant positive correlation was found between Cd

15   content and expression levels of *FlHMA3* in roots of *F. loliaceum* exposed to either 25

16   or 100 mg L^{-1} $CdCl_2$ concentrations within the 3–168 h time frame (Figs. 5B–6B).

17   This result provides supporting evidence to suggest an association between Cd

18   tolerance and *FlHMA3* expression in *F. loliaceum*.

19

20

21

22

15

1 **4. Discussion**

2   P_{1B}-ATPases are involved in heavy metal transport through biological membranes

3 via an ATP-dependent process. P_{1B2}-ATPases, which are unique to plants and have

4 attracted much attention, play a critical role in controlling the translocation of Zn^{2+} or

5 Cd^{2+} from roots to shoots and in sequestration of Cd^{2+} from the cytoplasm into the

6 vacuole (Cobbett et al., 2003; Morel et al., 2009; Mendoza-Cózatl et al., 2011).

7 However, studies of similar proteins in non-model plants have been lacking. In this

8 paper, we have presented the first characterization of a homologous P_{1B2}-ATPase from

9 a synthetic hybrid of the forage grass species *F. loliaceum*, an amphiploid species

10 hybrid of the agricultural grasses *Lolium perenne* and *Festuca pratensis*. FlHMA3 has

11 amino acid homologies of 54% and 77%, respectively, with AtHMA3 of *A. thaliana*

12 and OsHMA3 of rice, both belonging to $Zn^{2+}/Cd^{2+}/Co^{2+}/Pb^{2+}$ transporting group of

13 P_{1B2}-ATPases (Gravot et al., 2004; Miyadate et al., 2011). The FlHMA3 polypeptide

14 sequence was found to possess the expected features of eight transmembrane domains

15 and a CPC motif. The motifs DKTGTLT, HP, and GDGxNDx shown in Fig. 1 are

16 considered to be the domains of ion transduction, phosphorylation, and translocation

17 of metal ions in the large cytoplasmic loop and for ATP binding. Similar motifs have

18 been reported for AtHMA3 from *A. thaliana* (Gravot et al., 2004), GmHMA8 from

19 soybean (Bernal et al., 2007), OsHMA3 from rice (Miyadate et al., 2011), TcHMA3

20 from *T. caerulescens* (Ueno et al., 2011), HvHMA2 from barley (Mills et al., 2012),

21 and CsHMA3/4 from cucumber (Migocka et al., 2015). The GxCCxxE motif, which

22 occurs in the N or C terminus of all plant P_{1B2}-ATPases, is generally thought to be

1   associated with a heavy-metal-binding domain (Williams and Mills, 2005; Mills et al.,

2   2010). In this study, a GxCCxxE motif was located in the N terminus of FlHMA3,

3   thereby implying the presence of a heavy-metal-associated domain in this region (Fig.

4   1). Overexpression of *OsHMA3* in a yeast mutant has been shown to affect sensitivity

5   to Cd^{2+} and the ability to transport Cd^{2+} into vacuoles, which indicates that *HMA3* is

6   responsible for sequestration of Cd^{2+} into vacuoles (Ueno et al., 2010; Miyadate et al.,

7   2011). The methodologies we employed to demonstrate that *FlHMA3* similarly

8   encodes a P_{1B2}-ATPases transporter involved in sequestration of Cd^{2+} into the vacuole.

9   First, we fused GFP to FlHMA3 to visualize the subcellular localization of the

10   protein in wild-type *A. thaliana* cells. Confocal imaging revealed that FlHMA3 is

11   specifically located on the vacuolar membrane (Fig. 2). Previous studies have found

12   that AtHMA3 and OsHMA3 are localized on vacuolar membranes and are involved in

13   transporting heavy metal ions from the cytoplasm into vacuoles (Gravot et al., 2004;

14   Ueno et al., 2010). The consistency observed in localization of FlHMA3 to vacuolar

15   membranes suggests a possible role for the protein in the transfer of Cd^{2+} from the

16   cytoplasm into the vacuole across the vacuolar membrane. Furthermore, gene

17   expression analysis indicated that *FlHMA3* was mainly expressed in roots of *F.*

18   *loliaceum* exposed to $CdCl_2$ stress (Fig. 3) as in the case of rice *OsHMA3* (Miyadate

19   et al., 2011). An equivalent functional role may also be anticipated for *FlHMA3* as a

20   determinant factor in the root in Cd tolerance. *FlHMA3* expression patterns in *F.*

21   *loliaceum* do reflect a possible adaptation response to $CdCl_2$ stress. Ueno et al. (2010)

22   reported that OsHMA3 from a low Cd^{2+} accumulating cultivar (Nipponbare) functions

1   as a firewall by sequestrating Cd^{2+} into the vacuoles of roots, thereby separating Cd^{2+}

2   from areal parts. A subsequent study confirmed that *OsHMA3* overexpression

3   enhances tolerance to Cd^{2+} toxicity by increasing sequestration of Cd^{2+} into the

4   vacuoles of root cells and then decreasing the translocation of toxic Cd^{2+} into shoots

5   (Sasaki et al., 2014). One likely explanation is that only a limited amount of Cd^{2+} is

6   loaded into the xylem from the root cells and subsequently translocated to the shoots

7   (Miyadate et al., 2011). We note that a significant positive correlation was found

8   between *FlHMA3* expression levels and Cd accumulation in roots of *F. loliaceum*

9   exposed to different concentrations of Cd $(10-100 \text{ mg L}^{-1})$ for 168 h or to 25 or 100

10   mg L^{-1} over the same time period (Figs. 4B–6B). This speculates that *FlHMA3* was

11   detoxification of Cd^{2+} in *F. loliaceum* cells by enhancing the sequestration of Cd^{2+}

12   into the vacuole.

13   Both shoots and roots of *F. loliaceum* plants reached their highest Cd contents at

14   the highest applied $CdCl_2$ concentration (100 mg L^{-1}). The effect of this high

15   concentration was morphologically reflected by a significant reduction in plant

16   growth compared with the other Cd treatments (Figs. S2 and 4A). Most

17   heavy-metal-accumulating plants generally exhibit slow growth rates, low biomass

18   accumulation, and a tendency for altered root morphologies and necrosis (Clemens,

19   2006). Although the use of *F. loliaceum* for bioremediation of polluted soils requires

20   further scrutiny, the pilot study described herein suggests that this grass hybrid has

21   potential in such an application. One limitation of the current study is that our Cd

22   treatments, although extremely concentrated and highly toxic to plant growth, were

1   only applied over 168 h. Future research using the same *F. loliaceum* cultivar should

2   include much longer exposures to Cd stress. Assuming the promising results reported

3   here are observed over a longer time period, this grass may be used simultaneously

4   for two functions: bioremediation of Cd-contaminated land and provision of fodder

5   for livestock (its original agricultural role). In the latter case, the uptake of Cd^{2+} into

6   the shoots would have to be negligible to prevent harm to animals or subsequent entry

7   into the food chain. An additional consideration is that other heavy metals are likely

8   to be present in Cd-contaminated soils; the impact of these on *F. loliaceum* has yet to

9   be assessed.

10 **5. Conclusion**

11   Our results demonstrate that *FlHMA3* encoding a P_{1B2}-ATPase is a tonoplast

12 transporter that may play important roles in the response of *F. loliaceum* to Cd stress.

13 Further research should focus on understanding the mechanism in detail by using

14 methods like mutation or gene silencing.

15

16

17

18

19

20

21

22

1 **Acknowledgements**

12

13

14

15

16

17

18

19

20

21

22

References

Andrés-Colás, N., Sancenon, V., Rodriguez-Navarro, S., Mayo, S., Thiele, D.J., Ecker, J.R., Puig, S., Penarrubia, L., 2006. The Arabidopsis heavy metal P-type ATPase HMA5 interacts with metallochaperones and functions in copper detoxification of roots. Plant J. 45, 225–236.

Becher, M., Talke, I.N., Krall, L., Kramer, U., 2004. Cross-species microarray transcript profiling reveals high constitutive expression of metal homeostasis genes in shoots of the zinc hyperaccumulator *Arabidopsis halleri*. Plant J. 37, 251–268.

Bernal, M., Testillano, P.S., Alfonso, M., Risueñõ, M.C., Picorel, R., Yruel, I., 2007. Identification and subcellular localization of the soybean copper P_{1B}-ATPase GmHMA8 transporter. J. Struct. Biol.158, 46–58.

Chao, D.Y., Silva, A., Baxter, I., Huang, Y.S., Nordborg, M., Danku, J., Lahner, B., Yakubova, E., Salt, D.E., 2012. Genome-wide association studies identify heavy metal ATPase3 as the primary determinant of natural variation in leaf cadmium in *Arabidopsis thaliana*. PLoS Genet. 8, e1002923.

Clemens, S., 2006. Toxic metal accumulation, responses to exposure and mechanisms of tolerance in plants. Biochimie 88, 1707–1719.

Cobbett, C.S., Hussain, D., Haydon, M.J., 2003. Structural and functional relationships between type 1B heavy meta-transporting P-type ATPases in *Arabidopsis*. New Phytol. 159, 315–321.

Colangelo, E.P., Guerinot, M.L., 2006. Put the metal to the petal: metal uptake and

transport throughout plants. Curr. Opin. Plant Biol. 9, 322–330.

Gallego, S.M., Pena, L.B., Barcia, R.A., Azpilicueta, C.E., Iannone, M.F., Rosales, E.P., Zawoznik, M.S., Groppa, M.D., Benavides, M.P., 2012. Unravelling cadmium toxicity and tolerance in plants: insight into regulatory mechanisms. Environ. Exp. Bot. 83, 33–46.

Gravot, A., Lieutaud, A., Verret, F., Auroy, P., Vavasseu, A., Richaud, P., 2004. AtHMA3, a plant P_{1B}-ATPase, functions as a Cd/Pb transporter in yeast. FEBS Lett. 561, 22–28.

Guo, Q., Wang, P., Ma, Q., Zhang, J.L., Bao, A.K., Wang, S.M., 2012. Selective transport capacity for K^+ over Na^+ is linked to the expression levels of *PtSOS1* in halophyte *Puccinellia tenuiflora*. Funct. Plant Biol.39, 1047–1057.

Guo, Q., Meng, L., Mao, P.C., Tian, X.X., 2014. An assessment of *Agropyron cristatum* tolerance to cadmium contaminated soil. Biol. Plant.58, 174–178.

Hanikenne, M., Nouet, C., 2011. Metal hyperaccumulation and hypertolerance: a model for plant evolutionary genomics. Curr. Opin. Plant Biol.14, 252–259.

Hirschi, K.D., Korenkov, V.D., Wilganowski, N.L., Wagner, G.J., 2000. Expression of *Arabidopsis CAX2* in tobacco altered metal accumulation and increased manganese tolerance. Plant Physiol. 124,125–133.

Humphreys, M.W., Thomas, H.M., Morgan, W.G., Meredith, M.R., Harper, J.A., Thomas, H., Zwierzykowski, Z., Ghesquiére, M., 1995. Discriminating the ancestral progenitors of hexaploid *Festuca arundinacea* using genomic in-*situ* hybridization. Heredity 75, 171–174.

1 Humphreys, M.W., O'Donovan, S.A., Farrell, M.S., Gay, A., Kingston-Smith, A.L.,

2   2014. The potential of novel *Festulolium* (2n=4x=28) hybrids as productive,

3   nutrient-use-efficient fodder for ruminants. Food Energy Secur. 50, 1–13.

4 Hussain, D., Haydon, M.J., Wang, Y., Wong, E., Sherson, S.M., Young, J., Camakaris,

5   J., Harper, J.F., Cobbett, C.S., 2004. P-type ATPase heavy metal transporters with

6   roles in essential zinc homeostasis in Arabidopsis. Plant Cell 16, 1327–1339.

7 Kim, Y.Y., Choi, H., Segami, S., Cho, H.T., Martinoia, E., Maeshima, M., Lee, Y.,

8   2009. AtHMA1 contributes to the detoxification of excess Zn (II) in Arabidopsis.

9   Plant J. 58, 737–753.

10 Korenkov, V., Hirschi, K., CrutchWeld, J.D., Wagner, G.J., 2007. Enhancing tonoplast

11   Cd/H antiport activity increases Cd, Zn, and Mn tolerance, and impacts root/shoot

12   Cd partitioning in *Nicotiana tabacum* L. Planta 226, 1379–1387.

13 Livak, K.J., Schmittgen, T.D., 2001. Analysis of relative gene expression data using

14   real-time quantitative PCR and the $2^{-\Delta\Delta CT}$ method. Methods 25, 402–408.

15 MacLeod, C.J.A., Humphreys, M.W., Whalley, R., Turner, L., Binley, A., Watts, C.W.,

16   Skot, L., Joynes, A., Hawkins, S., King, I.P., O'Donovan, S., Haygarth, P.M.,

17   2013. A novel grass hybrid to reduce flood generation in temperate regions. Sci

18   Rep. 3, 1683.

19 Martínez, J.P., Kinet, J.M., Bajji, M., Lutts, S., 2005. NaCl alleviates polyethylene

20   glycol-induced water stress in the halophyte species *Atriplex halimus* L. J. Exp.

21   Bot. 419, 2430–2431.

22 Mendoza-Cózatl, D., Loza-Tavera, H., Hernández-Navarro, A., Moreno-Sánchez, R.,

23

2005. Sulfur assimilation and glutathione metabolism under cadmium stress in yeast, protists and plants. FEMS Microbiol. Rev. 29, 653–671.

Mendoza-Cózatl, D.G., Jobe, T.O., Hauser, F., Schroeder, J.I., 2011. Long distance transport, vacuolar sequestration, tolerance, and transcriptional responses induced by cadmium and arsenic. Curr. Opin. Plant Biol. 14, 554–562.

Migocka, M., Papierniak, A., Maciaszczyk-Dziubinska, E., Posyniak, E., Kosieradzka, A., 2015. Molecular and biochemical properties of two P_{1B2}-ATPases, CsHMA3 and CsHMA4, from cucumber. Plant Cell Environ. 38, 1127–1141.

Mills, R.F., Valdes, B., Duke, M., Peaston, K.A., Lahner, B., Salt, D.E., Williams, L.E. 2010. Functional significance of AtHMA4 C-terminal domain in planta. PLoS One 5, e13388.

Mills, R.F., Peaston, K.A., Runions, J., Williams, L.E., 2012. HvHMA2, a P_{1B}-ATPase from Barley, is highly conserved among cereals and functions in Zn and Cd transport. PLoS One 7, e42640.

Miyadate, H., Adachi, S., Hiraizumi, A., Tezuka1, K., Nakazawa, N., Kawamoto, T., Katou, K., Kodama, I., Sakurai, K., Takahashi, H., Satoh-Nagasawa, N., Watanabe, A., Fujimura, T., Akagi, H., 2011. *OsHMA3*, a P_{1B}-type of ATPase affects root-to-shoot cadmium translocation in rice by mediating efflux into vacuoles. New Phytol. 189, 190–199.

Morel, M., Crouzet, J., Gravot, A., Auroy, P., Leonhardt, N., Vavasseur, A., Richaud, P., 2009. AtHMA3, a P_{1B}-ATPase allowing Cd/Zn/Co/Pb vacuolar storage in Arabidopsis. Plant Physiol.149, 894–904.

1   Peralta-Videa, J.R., Lopez, M.L., Narayan, M., Saupe, G., Gardea-Torresdey, J., 2009.

2   The biochemistry of environmental heavy metal uptake by plants: implications

3   for the food chain. Int. J. Biochem. Cell B. 41, 1665–1677.

4   Satoh-Nagasawa, N., Mori, M., Nakazawa, N., Kawamoto, T., Nagato, Y., Sakurai, K.,

5   Takahashi, H., Watanabe, A., Akagi, H., 2012. Mutations in rice (*Oryza sativa*)

6   heavy metal ATPase 2 (*OsHMA2*) restrict the translocation of zinc and cadmium.

7   Plant Cell Physiol. 53, 213–224.

8   Sasaki, A., Yamaji, N., Ma, J.F., 2014. Overexpression of *OsHMA3* enhances Cd

9   tolerance and expression of Zn transporter genes in rice. J. Exp. Bot. 65,

10 6013–6021.

11 Song, W.Y., Sohn, E.J., Martinoia, E., Yong, Y.Y., Jasinski, M., Forestier, C., Hwang,

12 I., Lee, Y., 2003. Engineering tolerance and accumulation of lead and cadmium in

13 transgenic plants. Nat. Biotechnol. 8, 914–919.

14 Takahashi, R., Bashir, K., Ishimaru, Y., Nishizawa, NK., Nakanishi, H., 2012. The

15 role of heavy-metal ATPases, HMAs, in zinc and cadmium transport in rice. Plant

16 Signal. Behav. 7, 1605–1607.

17 Tamura, K., Peterson, D., Peterson, N., Stecher, G., Nei, M., Kumar, S., 2011.

18 MEGA5: molecular evolutionary genetics analysis using maximum likelihood,

19 evolutionary distance, and maximum parsimony methods. Mol. Biol. Evol. 28,

20 2731–2739.

21 Thompson, J.D., Gibson, T.J., Plewniak, F., Jeanmougin, F. Higgins, D.G., 1997. The

22 ClustalX windows interface: flexible strategies for multiple sequence alignment

aided by quality analysis tools. Nucleic. Acids Res. 24, 4876–4882.

Ueda, T., Yamaguchi, M., Uchimiya, H., Nakano, A., 2001. *Ara6*, a plant-unique novel type Rab GTPase, functions in the endocytic pathway of *Arabidopsis thaliana*. EMBO J. 20, 4730–4741.

Ueno, D., Yamaji, N., Kono, I., Huang, C.F., Ando, T., Yano, M., Ma, J.F., 2010. Gene limiting cadmium accumulation in rice. Proc. Natl Acad. Sci. USA. 107, 16500–16505.

Ueno, D., Milner, M.J., Yamaji, N., Yokosho, K., Koyama, E., Clemencia Zambrano, M., Kaskie, M., Ebbs, S., Kochian, L.V., Ma, J.F., 2011. Elevated expression of *TcHMA3* plays a key role in the extreme Cd tolerance in a Cd-hyperaccumulating ecotype of *Thlaspi caerulescens*. Plant J. 66, 852–862.

Verbruggen, N., Hermans, C., Schat, H., 2009. Mechanisms to cope with arsenic or cadmium excess in plants. Curr. Opin. Plant Biol.12, 364–372.

Williams, L.E., Mills, R.F., 2005. P_{1B}-ATPases-an ancient family of transition metal pumps with diverse functions in plants. Trends Plant Sci.10, 491–502.

Wojas, S., Hennig, J., Plaza, S., Geisler, M., Siemianowski, O., Sklodowska, A., Ruszczyńska, A., Bulska, E., Antosiewic, D.M., 2009. Ectopic expression of Arabidopsis ABC transporter MRP7 modifies cadmium root-to-shoot transport and accumulation. Environ. Pollut. 157, 2781–2789.

Yoo, S.D., Cho, Y. H., Sheen, J., 2007. Arabidopsis mesophyll protoplasts: a versatile cell system for transient gene expression analysis. Nat. Protoc. 2, 1565–1572.

1 **Figure Legends**

2 **Fig. 1.** Sequence alignment of FlHMA3 with other HMA3s from higher plants.

3 Sources of P_{1B2}-ATPases and their GenBank accession numbers are as follows:

4 AtHMA3 (*Arabidopsis thaliana*, NM_119158), OsHMA3 (*Oryza sativa*,

5 XM_015791882), and TaHMA3 (*Triticum aestivum*, KF683298). The sequences were

6 aligned using DNAMAN 8.0 software. Amino acid residues highlighted in black are

7 conserved in the three transporters. Identical and different amino acid residues are

8 indicated with white and blue, respectively. Eight putative transmembrane domains

9 (TM 1–TM 8) and several motifs are boxed.

10 **Fig. 2.** Subcellular localization of an FlHMA3-GFP fusion protein transiently

11 expressed in *Arabidopsis thaliana* mesophyll cells. (A) Images obtained using GFP

12 alone as the control. The red dye FM 4-64 was used to indicate the plasma membrane

13 location. (B) Images obtained when GFP was fused to the C terminus of FlHMA3. In

14 panels A and B from left to right, GFP signals, FM 4-64 signals, merged images of

15 GFP and FM 4-64 signals, and bright-field differential interference contrast (DIC)

16 images are shown. Bar = 5 µm.

17 **Fig. 3.** *FlHMA3* expression in *F. loliaceum* exposed to (A) different concentrations of

18 $CdCl_2$ (0, 10, 25, 50, and 100 mg L^{-1}) for 168 h or to 25 mg L^{-1} $CdCl_2$ (B) or 100 mg

19 L^{-1} $CdCl_2$ (C) over a 168-h period. The relative expression level of *FlHMA3* in shoots

20 and roots was analyzed by quantitative real-time RT-PCR. *Actin* was used as an

21 internal control. Experiments were repeated three times. Data are means ± SD (n = 3)

22 and bars indicate SD. Different letters indicate significant differences at $P < 0.05$

23 (Duncan's test).

1   **Fig. 4.** Cd content of tissues of *F. loliaceum* exposed to 10, 25, 50, and 100 mg L^{-1}

2   CdCl$_2$ for 168 h. (A) Cd content of shoots and roots. Five plants were pooled per

3   replicate (*n* = 8). (B) Relationship between relative *FlHMA3* expression and Cd

4   content of roots subjected to 10 (♦), 25 (▲), 50 (■), and 100 (●) mg L^{-1} CdCl$_2$

5   treatment for 168 h (*n* = 3–8). Data are means ± SD and bars indicate SD. Different

6   letters indicate significant differences at *P* < 0.05 (Duncan's test).

7   **Fig. 5.** Time course of Cd content of *F. loliaceum* exposed to 25 mg L^{-1} CdCl$_2$ for 3 to

8   168 h. (A) Cd content of shoots and roots. Five plants were pooled per replicate (*n* =

9   8). (B) Relationship between relative *FlHMA3* expression and Cd content of roots

10   subjected to 25 mg L^{-1} CdCl$_2$ treatment for 3–168 h. Data are means ± SD (*n* = 3–8)

11   and bars indicate SD.

12   **Fig. 6.** Time courses of Cd content of *F. loliaceum* exposed to 100 mg L^{-1} CdCl$_2$ for 3

13   to 168 h. (A) Cd content of shoots and roots. Five plants were pooled per replicate (*n*

14   = 8). (B) Relationship between relative *FlHMA3* expression and Cd content of roots

15   subjected to 100 mg L^{-1} CdCl$_2$ treatment for 3–168 h. Data are means ± SD (*n* = 3-8)

16   and bars indicate SD.

17   **Supplementary Figure Legends**

18   **Supplementary Fig. 1.** Phylogenetic tree of *HMAs*. The tree was constructed by the

19   neighbor-joining method. Genes and GenBank accession numbers are as follows:

20   *AdHMA3* (*Arachis duranensis*, XM_016078710), *AiHNA3* (*Arachis ipaensis*,

21   XM_016346129), *AhHMA3* (*Arabidopsis halleri*, AJ556182), *AhHMA4* (*Arabidopsis*

22   *halleri*, AY960757), *AtHMA2* (*Arabidopsis thaliana*, NM_119157), *AtHMA3*

28

(*Arabidopsis thaliana*, NM_119158), *AtHMA4* (*Arabidopsis thaliana*, AF412407),

BdHMA3 (*Brachypodium distachyon*, XM_003561234), *BnHMA3* (*Brassica napus*,

XM_013849300), *BrHMA3* (*Brassica rapa*, XM_009139644), *CaHMA3* (*Cicer

arietinum*, XM_012717947), *CsHMA3* (*Camelina sativa*, JX402100), *CmHMA3*

(*Cucumis melo*, XM_008455480), *EgHMA3* (*Elaeis guineensis*, XM_010928912),

EugHMA3 (*Eucalyptus grandis*, XM_010048654), *ErgHMA3* (*Erythranthe guttata*,

XM_012995791), ●*FlHMA3* (*Festulolium loliaceum*), *FvHMA3* (*Fragaria vesca*,

XM_011464053), *GmHMA3* (*Glycine max*, XM_006593460), *GrHMA3* (*Gossypium

raimondii*, XM_012589041), *HvHMA2* (*Hordeum vulgare*, GU177852), *HvHMA3*

(*Hordeum vulgare*, KU212808), JcHMA3 (*Jatropha curcas*, XM_012211439),

MaHMA3 (*Musa acuminata*, XM_009417251), *MnHM3* (*Morus notabilis*,

XM_010112413), *NbHMA3* (*Nicotiana tabacum*, XM_016654239), *NcHMA4*

(*Noccaea caerulescens*, JQ904704), *ObHMA3* (*Oryza brachyantha*, XM_006658354),

OsHMA2 (*O. sativa*, HQ646362), *OsHMA3* (*O. sativa*, XM_015791882), PdHMA3

(*Phoenix dactylifera*, XM_008803179), *PeHMA3* (*Populus euphratica*,

XM_011021683), *PmHMA3* (*Prunus mume*, XM_008225567), *RcHMA3* (*Ricinus

communis*, XM_015727254), *SaHMA2* (*Sedum alfredii*, JQ012929), *SbHMA3*

(*Sorghum bicolor*, XM_002459533), *SiHMA3* (*Setaria italica*, XM_012843843),

SlHMA3 (*Solanum lycopersicum*, XM_004242795), *TaHMA2* (*Triticum aestivum*,

HM021132), *TaHMA3* (*Triticum aestivum*, KF683298), *ThHMA3* (*Tarenaya

hassleriana*, XM_010550291), *TtHMA3* (*Triticum turgidum*, KF683295), *VvHMA3*

(*Vitis vinifera*, XM_010658478), and *ZmHMA3* (*Zea mays*, XM_008671782).

1   **Supplementary Fig. 2.** Relative growth rate (RGR) of *F. loliaceum* exposed to 0, 10,

2   25, 50, or 100 mg L^{-1} $CdCl_2$ for 168 h. Five plants were pooled per replicate ($n = 8$).

3   Data are means ± SD and bars indicate SD. Different letters indicate significant
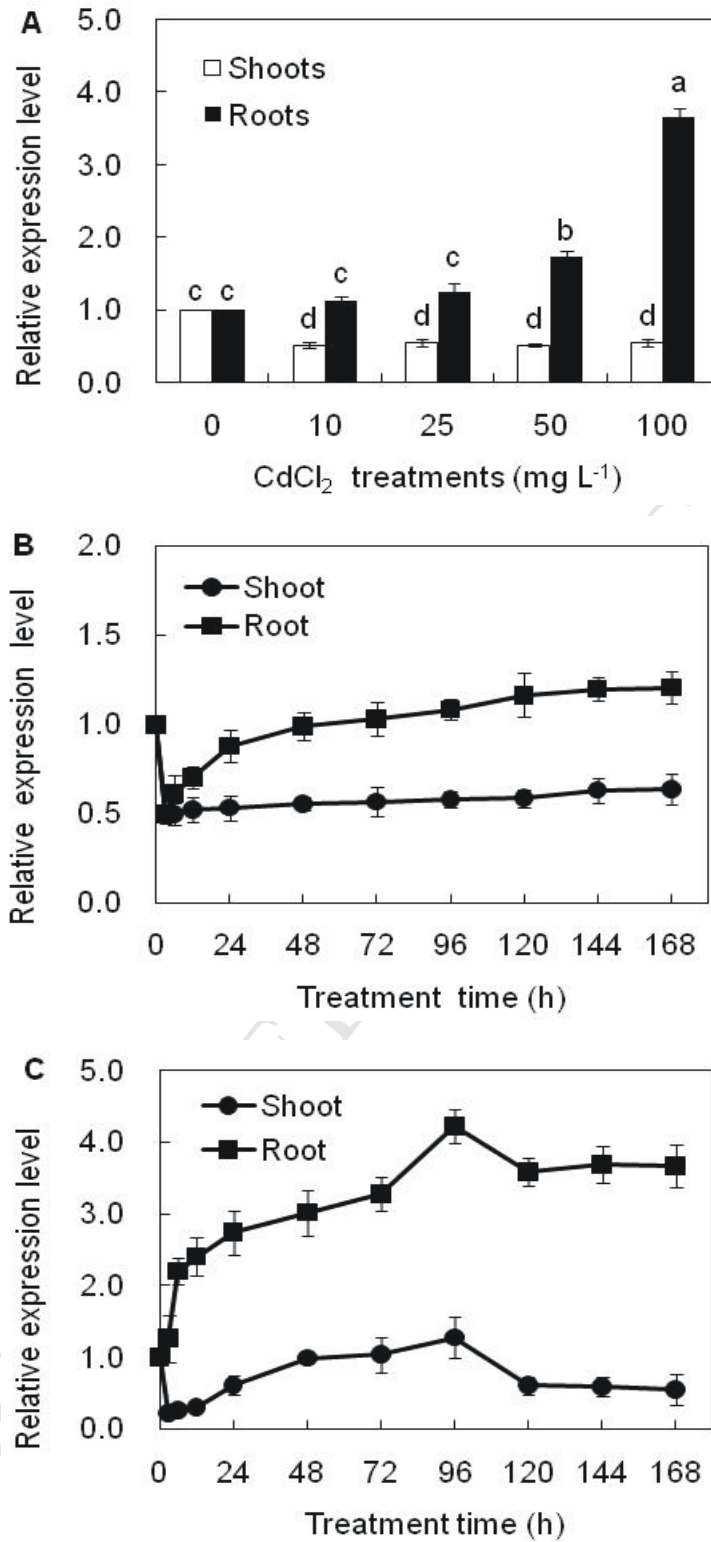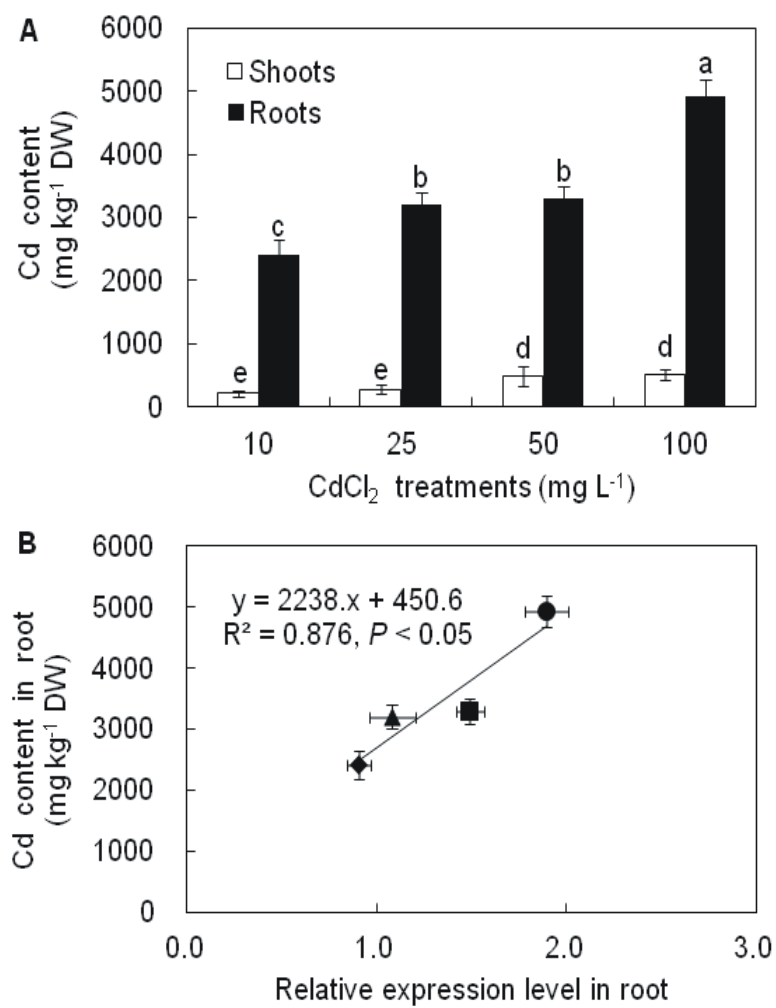
4   differences at $P < 0.05$ (Duncan's test).
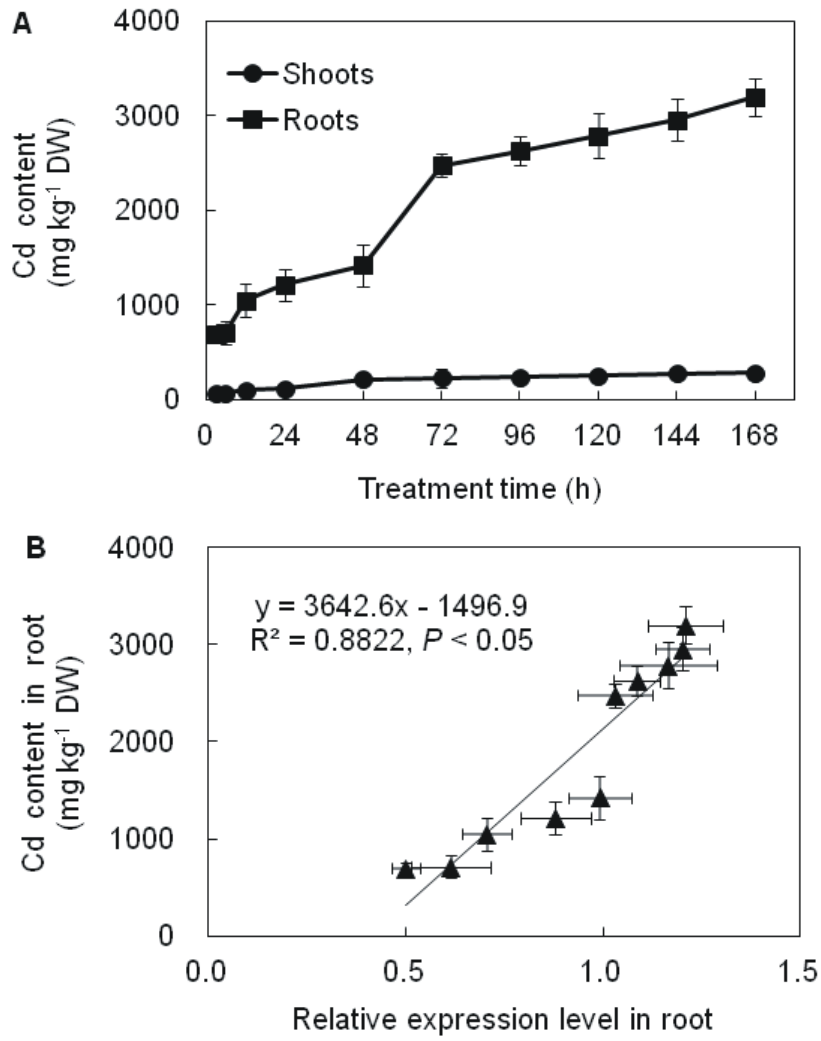
Fig. 1
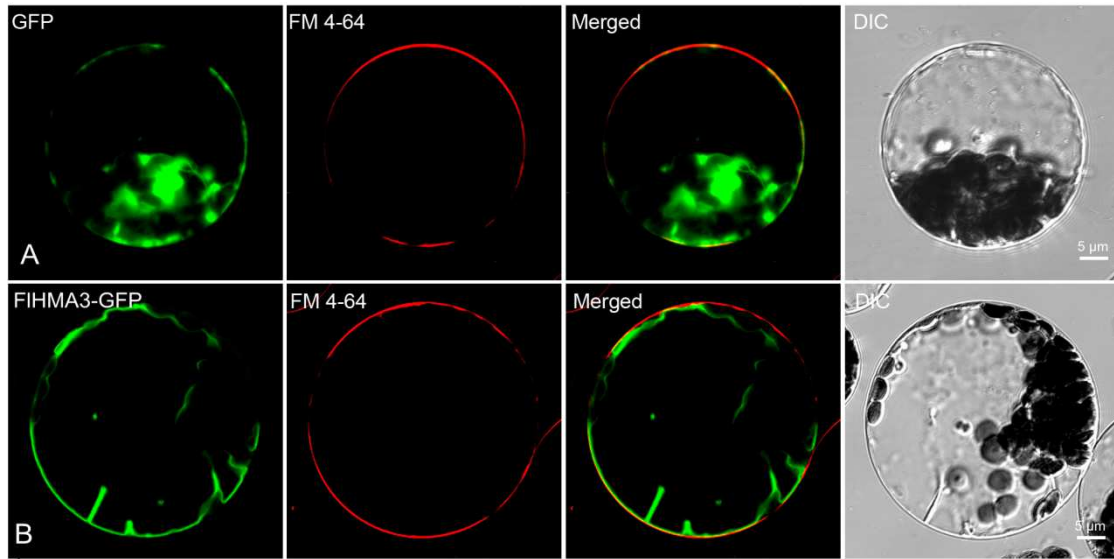
Fig. 2
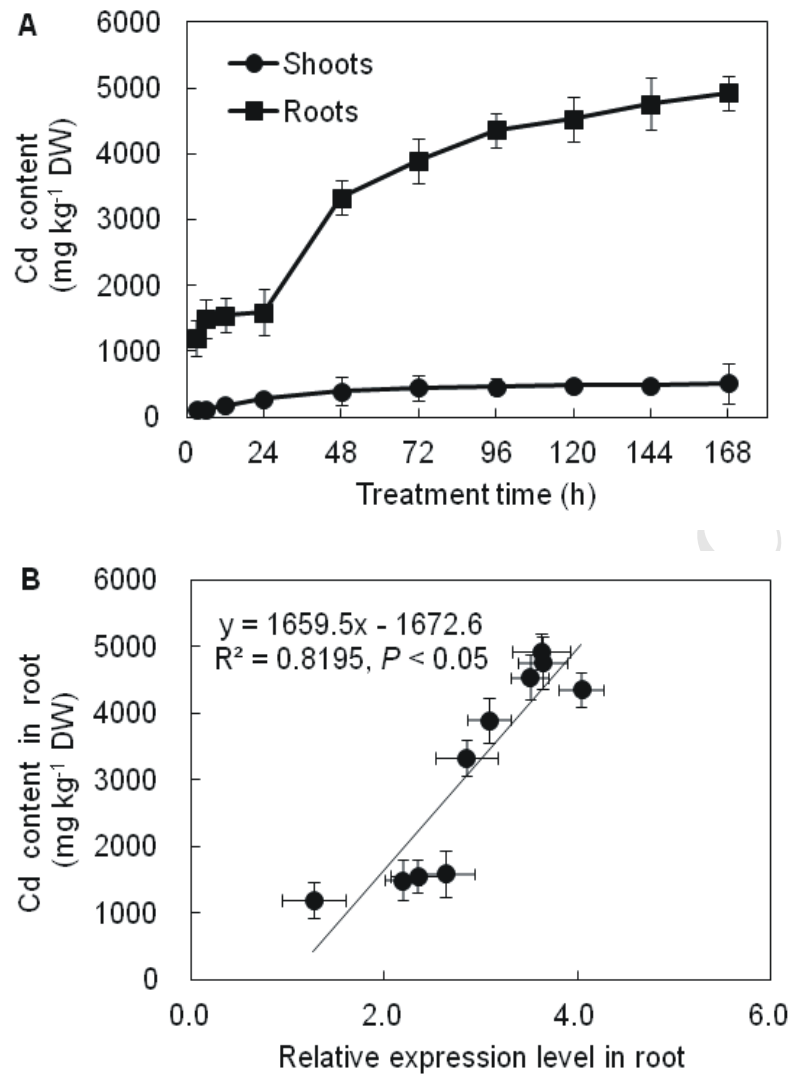
Fig. 3

Fig. 4

Fig. 5

Fig. 6

Supplementary Fig. 1
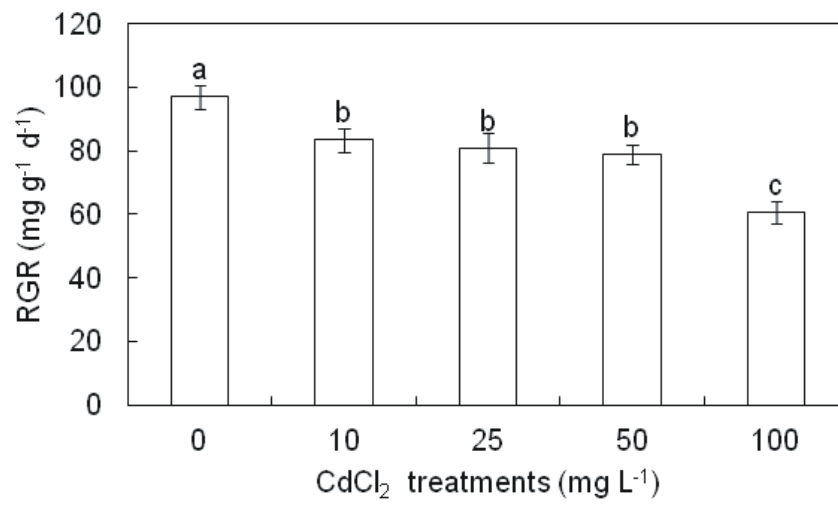
37

Supplementary Fig. 2

Supplementary Table 1

Primer sequences used in the experiments

Primer	Sequence (5'-3')
P1	ATCAACRTYCTSATGCTYATCGC
P2	GGTGATSGTSCCGGTCTTGTCGA
P3	GGTTACATTGCCGTGAGGACGAC
P4	TCGACAAGACCGGCACCATCACC
P5	GGG<u>GAATTC</u>ATGACGGACGGTGGCGAGAAC
P6	GGG<u>GGTACC</u>GTTTCACCAGAGCAGCATCCT
P7	GCTCAACCTGGACGGTTACA
P8	AACCATCGCTCCAGATCACC
A1	TCGAGACTGCGAAGAGTAGC
A2	TCCATGCCGATGATGGAAGG

Highlights

● *FlHMA3* was mainly expressed in roots and up-regulated by excess Cd.

● FlHMA3 was localized at the vacuolar membrane.

● A significant positive correlation was found between expression levels of *FlHMA3* and Cd accumulations in roots of *F. loliaceum* under Cd stress.

●Cd^{2+} taken up by root cells may be sequestered into the vacuole via a pathway mediated by FlHMA3 to reduce the concentration of this toxic metal in the cytoplasm.

Author contributions

Qiang Guo, Lin Meng and Mike W. Humphreys conceived and designed the experiments. Qiang Guo performed all the experiments and wrote the manuscript. John Scullion and Luis A.J. Mur review and polish the manuscript.